ORIGINAL RESEARCH ARTICLE

The Effect of β Stabilizers on the Structure and Energy of α/β Interfaces in Titanium Alloys

M.A. MURZINOVA, S.V. ZHEREBTSOV, D.N. KLIMENKO, and S.L. SEMIATIN

The structure and energy associated with interfaces between the BCC and HCP lattices (β and α phase, respectively) in titanium alloys with commonly used β stabilizers were analyzed. For this purpose, the crystallographic structure of the matching facets of broad, side and end faces was described using misfit dislocations and structural ledges which compensate the mismatch in atomic spacing of the α and β phases. The effect of the β/α transformation temperature due to various concentration of β stabilizers on periodicity of misfit dislocations and structural ledges was estimated. The van der Merwe approach was used to calculate energy of different matching facets. An increase in the percentage of β-stabilizing elements was found to result in a decrease in the lattice-parameter ratio (a_β/a_α) and an increase in the energy of all faces. The dependence of the interface energy on the a_β/a_α ratio was for the first time quantified, and insight into the preferred shape of α-phase precipitates was obtained.

https://doi.org/10.1007/s11661-021-06175-y

I. INTRODUCTION

SINCE most structural titanium alloys contain β-stabilizing elements, they usually consist of a high temperature β phase with a body-centered cubic (BCC) lattice and a low temperature α phase with a hexagonal close-packed (HCP) lattice. The proportion and morphology of the phases (*i.e.*, size, shape, preferential sites of precipitation, crystallographic orientation with respect to the matrix, *etc.*), which determine mechanical and physical properties, can be controlled by thermomechanical treatment.[1–5] In addition, the phase morphology depends on thermodynamic parameters of the system such as the elastic strain energy per unit volume of the new phase and the α/β interface energy per unit area.[6–8] For example, the lamellar shape of the α phase constituent in the β matrix in titanium alloys and the high stability of the lamellar structure during heat treatment are usually associated with the low energy of the broad face of α platelets and the high level of interface-energy anisotropy.[4,7–12]

There are no direct methods for measuring the energy of interfaces between different phases in multiphase alloys. Therefore, indirect methods or theoretical calculations are often used.[6–8] In the latter case, the chemical and structural components of the interface energy should be distinguished. The *chemical* component is associated with the bond energy between different species of atoms; the contribution of this component to the total interface energy increases with an increase in the difference in the chemical composition of the phases. If the phases differ from each other in both composition and crystal (lattice) type, the main contribution to the interface energy is usually associated with the *structural*, component. This structural component depends on the length of facets with coherent matching and the type and density of structural defects along the interface at which elastic stresses generated at the coherent parts can be relaxed. The structural defects usually include misfit dislocations (MDs) and structural ledges. Model approximations of partly-coherent interface structures containing these defects have been proposed previously.[13–16] To the present, a number of the model approximations/assumptions have been confirmed experimentally via high-resolution electron microscopy, for example.[8,17–27]

Several approaches have been developed to quantify the energy of either planar interfaces, for which the mismatch is compensated by arrays of edge and screw MDs,[13] or interfaces with structural ledges.[28,29] These approaches have been summarized previously.[8] The key inputs for such evaluations comprise: (i) the crystallographic indices of the matching planes and directions of both phases at the interface, (ii) the lattice

M.A. MURZINOVA is with the Institute for Metals Superplasticity Problems, Russian Academy of Sciences, Khalturin 39, Ufa, Russia 450001. Contact e-mail: mma@imsp.ru S.V. ZHEREBTSOV and D.N. KLIMENKO are with the Belgorod National Research University, Pobeda 85, Belgorod, Russia 308015. S.L. SEMIATIN is with the Air Force Research Laboratory, Materials & Manufacturing Directorate, Wright-Patterson Air Force Base, OH 45433-7817.
Article published online March 9, 2021

parameters of the phases, and (iii) the elastic moduli of the phases.

A structural model for the energy of the *broad face* between α lamellae and the β matrix in titanium alloys, containing arrays of MDs and structural ledges,[16,20,30] and an algorithm for the calculation of energy[28,29] were developed and applied in Reference 31 for Ti-6Al-4V as a function of temperature. Earlier results[32] for the high-temperature lattice parameters of the α and β phases of this alloy, the chemical composition of the phases, and the influence of temperature and phase composition on elastic moduli were taken into account. The structural component of the broad-face energy was found to depend noticeably on the chemical composition of the phases.[31] Specifically, the composition of the α phase in Ti-6Al-4V does not change noticeably with a decrease in temperature from 975 °C to 600 °C, but the vanadium content increases and the lattice parameter decreases markedly for the β phase over this temperature interval.[32] As a result, the spacing of the edge MDs decreases and the energy of the broad α/β interface increases gradually thereby approaching that of a high-angle grain boundary.[31]

A similar effect of other β-stabilizing elements, which partition to the β phase and decrease its lattice parameter, on the structure and energy of the broad face can be expected. Hence, it may be hypothesized that some alloying elements (and $\beta \rightarrow \alpha$ transformation conditions) may result in the loss of coherency at the broad face and a considerable decrease in the interface-energy anisotropy. This can lead to instability of the lamellar shape of the α phase precipitating in the β matrix of titanium alloys during diffusional transformations. The aim of the present work, therefore, was to determine the nature of α/β interfaces (lattice mismatch, average spacing between MDs and/or structural ledges along the mating facets) and to evaluate the effect of substitutional β-stabilizing elements on the interface energy in two-phase titanium alloys.

II. CRYSTALLOGRAPHY OF α/β INTERFACES

The results of numerous experiments and simulations[10–29] have revealed the characteristic features of the interface between the α lamellae and the β matrix in two-phase (α/β) titanium alloys (Figure 1):

(1) The crystal lattices of the α and β phases satisfy the Burgers orientation relationship (OR): $(0001)_\alpha || (110)_\beta$, $[\bar{2}110]_\alpha || [\bar{1}11]_\beta$, and $[0\bar{1}10]_\alpha || [1\bar{1}2]_\beta$. Growth ledges are observed on all interfaces (broad, side, and end faces). Both the horizontal and vertical rising surfaces of the growth ledges are usually formed by crystallographic planes with low Miller indices. The spacing between the growth ledges varies from tens to hundreds of nanometers.[18–23] The growth direction and the broad and end faces have macroscopically irrational Miller indices.[10,11,16–27]

(2) Each of the three faces of an α lamella has a partly-coherent structure with a varying level of coherency.[17–26] Arrays of MDs are present on all surfaces; the MDs can form loops around the α lamellae.[20,26] The MDs (which can be both perfect and partial) compensate for the mismatch in atomic spacing and/or deviations from the parallelism of the conjugate planes at the interface.

(3) The best match along the broad face of the α/β interface is ensured by structural ledges. They are spaced several (1 to 4) nm apart and are only ~ 0.25-nm high.[19,27]

A possible arrangement of the BCC and HCP lattices obeying the Burgers OR is shown in Figure 2. The crystallographic planes forming the matching facets on different faces and the directions corresponding to the Burgers vectors of the MDs are shown in Table I.

A broad face with structural ledges is shown schematically in the upper right part of Figure 1; the atomic structure of such a boundary has been described before.[30,31] Terraces of the structural ledges are formed by the $(0\bar{1}10)_\alpha || (1\bar{1}2)_\beta$ planes. On terrace planes, the interatomic mismatch in the $\mathbf{b_1} = 1/3[\bar{2}\,110]_\alpha || 1/2[\bar{1}\,11]_\beta$ direction is accommodated by structural ledges; and in the $\mathbf{b_2} = [0001]_\alpha || [110]_\beta$ direction by edge dislocations (Figures 1 and 2, Table I), which can split into partial dislocations.[19,20,25,26] Edge dislocations with the Burgers vector $\mathbf{b_z}$ accommodate the mismatch in the $[0\,\bar{1}\,1\,0]_\alpha || [1\,\bar{1}\,2]_\beta$ direction. These mismatches are associated with tensile or compression elastic stresses normal to the terrace plane. In References 28, 29, these dislocations were referred to as tilt misfit dislocations (TMDs).

Facets formed by either $(0001)_\alpha || (110)_\beta$ close-packed planes and two arrays of MDs with Burgers vectors $\mathbf{b_1}$ and $\mathbf{b_4}$ (Table I) or $(0\bar{1}11)_\alpha$ ∠~ 1.4 deg $(101)_\beta$ planes in which the mismatch is accommodated by perfect and partial dislocations with the Burgers vectors $\mathbf{b_1}$ and $\mathbf{b_5}$, respectively (Table I), are observed on the side face. On the end face, the matching facets comprise pairs of $(1\,\bar{1}\,00)_\alpha$ and $(1\,\bar{1}\,0)_\beta$ planes (with MDs having the Burgers vectors $\mathbf{b_2}$ and $\mathbf{b_4}$) or $(1\bar{1}0\bar{1})_\alpha$ and $(3\bar{1}0)_\beta$ planes

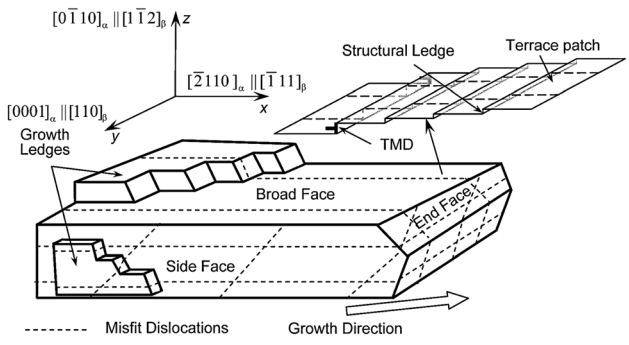

Fig. 1—Schematic illustration of α/β interfaces in titanium alloys (compiled from Refs. 10,12,14–27).

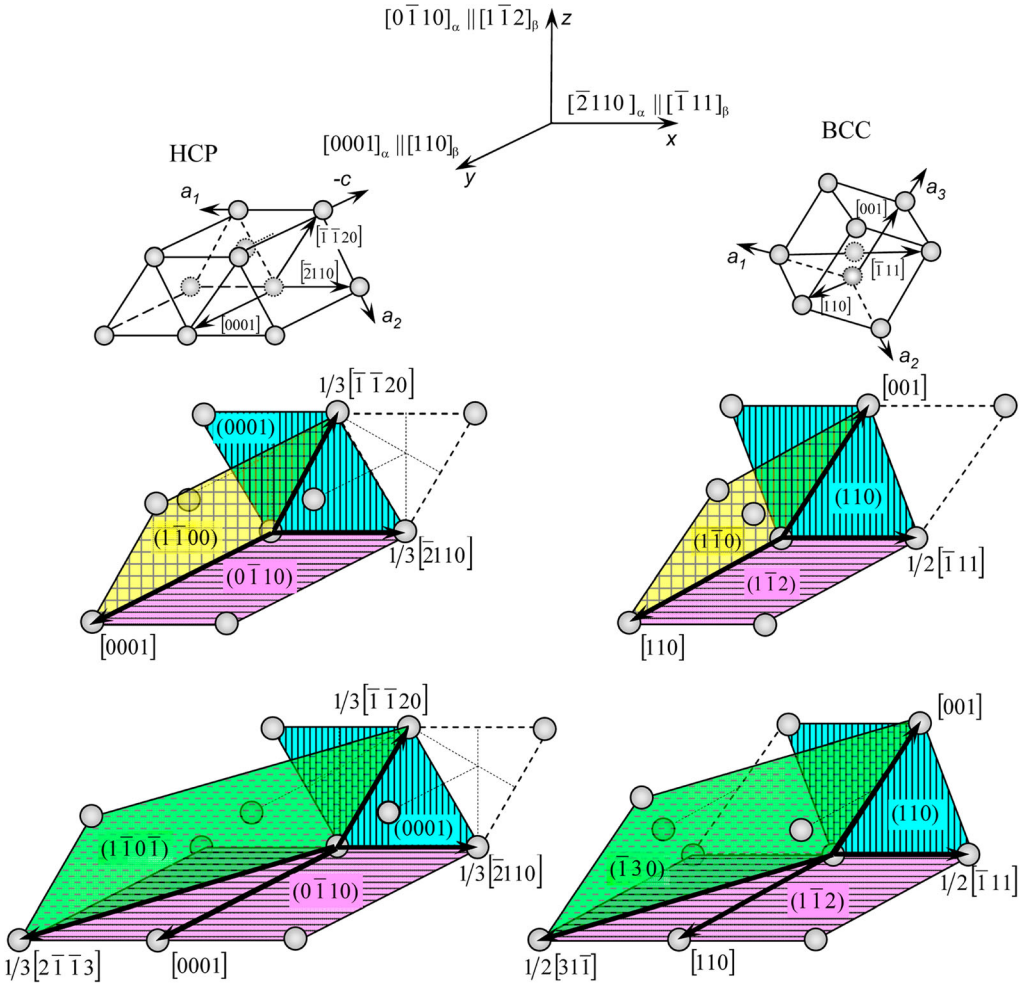

Fig. 2—Arrangement of the BCC and HCP lattices obeying the Burgers OR.

Table I. Matching Planes and Directions Between the BCC and HCP Lattice per the Burgers OR

Type	Planes Forming the Matching Facets	Burgers Vectors of MDs
Broad face		
I	$(0\bar{1}10)_\alpha \| (1\bar{1}2)_\beta$	$\mathbf{b_1} = 1/3[\bar{2}110]_\alpha \| 1/2[\bar{1}11]_\beta$ and $\mathbf{b_2} = [0001]_\alpha \| [110]_\beta$
II		$\mathbf{b_3} = 1/3[2\bar{1}\bar{1}3]_\alpha \| 1/2[31\bar{1}]_\beta$
Side face		
III	$(0001)_\alpha \| (110)_\beta$	$\mathbf{b_1} = 1/3[\bar{2}110]_\alpha \| 1/2[\bar{1}\ 11]_\beta$
		$\mathbf{b_4} = 1/3[\bar{1}\bar{1}20]_\alpha \angle \sim 5.3$ deg $[001]_\beta$
IV	$(0\bar{1}11)_\alpha \angle \sim 1.4^\circ (101)_\beta$	$\mathbf{b_1} = 1/3[\bar{2}110]_\alpha \| 1/2[\bar{1}11]_\beta$
		$\mathbf{b_5} = 1/6[11\bar{2}3]_\alpha \angle \sim 3.1$ deg $1/2[11\ \bar{1}]_\beta$
End face		
V	$(1\bar{1}00)_\alpha \angle \sim 5.3^\circ (1\bar{1}0)_\beta$	$\mathbf{b_2} = [0001]_\alpha \| [110]_\beta$
		$\mathbf{b_4} = 1/3[\bar{1}\bar{1}20]_\alpha \angle \sim 5.3$ deg $[001]_\beta$
VI	$(1\bar{1}0\bar{1})_\alpha \angle \sim 5.1^\circ (\bar{1}30)_\beta$	$\mathbf{b_3} = 1/3[2\bar{1}\bar{1}3]_\alpha \angle \sim 5.6$ deg $1/2[31\bar{1}]_\beta$
		$\mathbf{b_4} = 1/3[\bar{1}\bar{1}20]_\alpha \angle \sim 5.3$ deg $[001]_\beta$
VII	$(10\bar{1}\bar{1})_\alpha \angle \sim 9.3^\circ (10\bar{1})_\beta$	$\langle \mathbf{b_1} \rangle = 1/3[1\bar{2}10]_\alpha$ and $1/2[1\bar{1}1]_\beta$
		$\langle \mathbf{b_3} \rangle = 1/3[\bar{2}113]_\alpha$ and $1/2[131]_\beta$
VIII	$(10\bar{1}0)_\alpha \angle \sim 10.5^\circ (\bar{1}12)_\beta$	$\langle \mathbf{b_1} \rangle = 1/3[1\bar{2}10]_\alpha \| 1/2[1\bar{1}1]_\beta$ and $\mathbf{b_2} = [0001]_\alpha \| [110]_\beta$
		$\langle \mathbf{b_3} \rangle = 1/3[1\bar{2}13]_\alpha$ and $1/2[311]_\beta$

$\angle$ denotes the angle θ between the most closely matching planes or directions in the BCC and HCP lattices.

(with Burgers vectors of the MDs being $\mathbf{b_3}$ and $\mathbf{b_4}$) (Figure 2, Table I). Because the matching planes and directions on the side and end faces are not parallel in most cases (Table I), the MDs contain both edge and screw components while the α/β interfaces contain tilt-compensation dislocations which eliminate the non-parallelism between the pairs of conjugate planes. It is worth noting that algorithms for estimating interface energy[8,13–15,28,29] do not properly consider the presence of partial and mixed-type dislocations at the matching facets. In the present work, however, attention is restricted to interfaces for which all of the mismatch can be accommodated by perfect dislocations, and the angles between the matching planes and directions do not exceed 6 deg. Pairs of planes that meet these conditions are colored identically in Figure 2.

III. EFFECT OF TEMPERATURE ON THE PHASE COMPOSITION, LATTICE PARAMETERS, INTERFACE STRUCTURE, AND ELASTIC PROPERTIES

A. *Effect of Temperature on the Composition and Lattice Parameters of the α and β Phases*

Results of earlier experiments[1,4,32–37] and analysis of pseudo-binary phase diagrams[1–3,38–45] suggest that once nucleated during cooling from the β field, α lamellae grow diffusionally. This diffusional growth can occur over a wide range of temperature. However, this growth results in relatively little change in the composition of the α phase while changes in the composition of the β phase are quite significant. For Ti-5.4Al-4.7V-1.9Mo-1.2Cr-0.5Fe, for example, the total concentration of β-stabilizers in the β phase has been found to increase from 6.7 at. pct in the initial condition to ~ 9 at. pct after annealing at 800 °C and up to 22 at. pct after long-term annealing at 550 °C. The β-stabilizer concentration in the α phase after annealing at 800 and 550 °C was 2.8 and 2.5 at. pct, respectively.[34,35] In Ti-6Al-4V, the concentration of vanadium in the β phase was ~ 4.2 at. pct after annealing at 975 °C and 15.4 at. pct after cooling to 600 °C[32]; the corresponding concentration of vanadium in the α phase was ~ 1.5 at. pct in both cases. Similar changes in the chemical composition of the phases are observed in other titanium alloys with β-stabilizing elements.[38–45]

β-stabilizing elements in titanium alloys are usually subdivided into β-isomorphous (Mo, Nb, Ta, V, W) and β-eutectoid (Cr, Cu, Fe, Mn, Si, Ni etc.) elements.[1–3] Some β-isomorphous elements (Nb and Ta) dissolve in the β phase completely (Figure 3(a)),[42,45] while others (Mo, V and W) cause a miscibility gap in the β phase, leading to a monotectoid reaction ($\beta(C_M) \rightarrow \alpha(C_{\alpha D}) + \beta(C_{\beta N})$, where C_M represents the monotectoid composition of the β phase (point M); $C_{\alpha D}$ and $C_{\beta N}$ are the respective compositions of the α and β phases (points D and N, respectively), Figure 3(b)) [5,41,43–46]. The eutectoid β-stabilizers form intermetallic compounds through a eutectoid reaction (Figure 3(c)).[38–40,45]

Some β-stabilizing elements in titanium alloys, their solubility in the α and β phases, and critical temperatures are listed in Table II. The data in Table II show that the β-stabilizer solubility in the α phase is less than 0.5 at. pct in most cases and does not exceed 3 at. pct. On the other hand, the solubility of β-stabilizers in the β phase can be tens of atomic percent. According to References 43 and 44, for instance, the concentration of W and V in the β phase in equilibrium with the α phase can reach 80 at. pct after an "infinitely-long" anneal at 720 °C and 650 °C, respectively. However, in Ti-V model alloys (in which the total amount of impurities is ≤ 0.3 pct), the concentration of vanadium in the β phase does not exceed 55 at. pct even after annealing at 650 °C for 4000 hours.[46]

A linear fit can be used as an approximate description of the increase in the concentration of component X in the β phase when temperature decreases from 882 °C to the values corresponding to points C, M and E (Figures 3(a), (b) and (c), respectively).

During cooling of an alloy Ti-X_1 (Figures 3(a) through (c)) from a temperature T_0 (β phase field) to T_1 ($\alpha + \beta$ phase field), the α phase precipitates in the parent β phase. At the early stages of the $\beta \rightarrow \alpha$ transformation, the composition of the β matrix far from the nucleated α particles is still essentially X_1, while near the α particles the concentration of β stabilizers increases.[7,8] A local equilibrium can exist at the α/β interface; at the temperature T_1, α phase with a composition $C_\alpha = X_{\alpha/\beta}(T_1)_{eq}$ is in thermodynamic equilibrium with β phase having a composition $C_\beta = X_{\beta/\alpha}(T_1)_{eq}$, per the phase diagram in Figure 3. (Note that the points $X_{\alpha/\beta}(T_1)_{eq}$ and $X_{\beta/\alpha}(T_1)_{eq}$ are not shown in Figure 3(b) to maintain the clarity of the illustration.)

In alloys X_1 and X_2 undercooled from T_0 to T_2, (where T_2 lies below the monotectoid line DMN), the α phase also precipitates in the β phase (Figure 3(b)). In this case, the content of β-stabilizers in the β phase in the vicinity of the α/β interface remains lower than the equilibrium level for a long time.[46] It can be assumed that the concentration of β stabilizers in the β phase increases gradually from $C_\beta = M$ to the equilibrium concentration $C_\beta = X_{\beta/\alpha}(T_2)_{eq}$, during an "infinity-long" soak at the (constant) temperature T_2, which is ~ 20 °C below the monotectoid temperature.

The lattice parameters of the equilibrium phases depend on both temperature and alloying-element content (Figure 4; vertical domains in Figure 4(a) show changes in the lattice parameter of the β phase during an "infinitely-long" annealing time at T_2 = const). Because experimental data on measurements of the high-temperature lattice parameters of the α and β phases are very limited, the lattice parameter of the β phase $a_\beta(C_\beta, T)$ with a β-stabilizer concentration of C_β at temperature T was determined using the expression [1]:

$$a_\beta(C_\beta, T) = a_\beta^{RT} + a_\beta^{RT} \times CTE \times 10^{-6}(T - 20), \quad [1]$$

in which a_β^{RT} is the room-temperature lattice parameter of material with a known concentration of β stabilizer(s) that has been solution-annealed above the solvus and then water-quenched,[1,45,47,48] CTE denotes

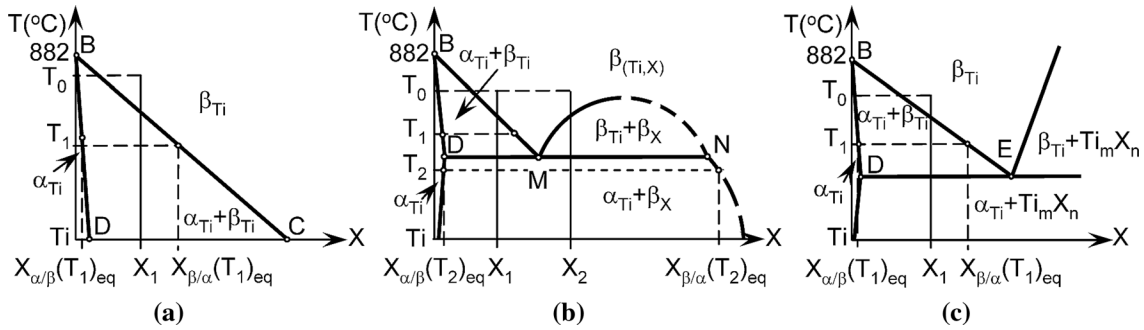

Fig. 3—Schematic phase diagrams for binary titanium alloys with different β-stabilizers: (*a*) β-stabilizers with complete solubility in the β phase, (*b*) β-stabilizers causing a miscibility gap in the β phase (monotectoid reaction), and (*c*) eutectoid systems in which intermetallic compounds are formed.

Table II. Solubility of Some Frequently Used β-Stabilizers in the α and β Phases[38–45]

β-Stabilizer	Nb	Ta	V	Mo	W	Mn	Cr	Fe	Cu
Type of β-Stabilizers	β-isomorphous elements					β-eutectoid elements			
Type of Interaction Between the β Matrix and β-Stabilizers	Complete solubility		Monotectoid reaction			Eutectoid reaction			
Temperature of Reaction (If Any), °C	—	—	675	695	740	550	667	580	800
Maximum Measured Solubility in the α-Phase, At. Pct	2.5 (400 °C)	3.0 (600 °C)	3.0	0.4	0.2	0.4	0.5	0.05	1.3
Measured Solubility in the β-Phase at Critical temperature, At. Pct	—	—	18.0	12.0	9.0	16.0	13.5	13.0	6.0
Predicted Solubility in the β-Phase at ~ 550 °C, At. Pct	50.0	70.0	80.0	60.0	70.0	—	—	—	—

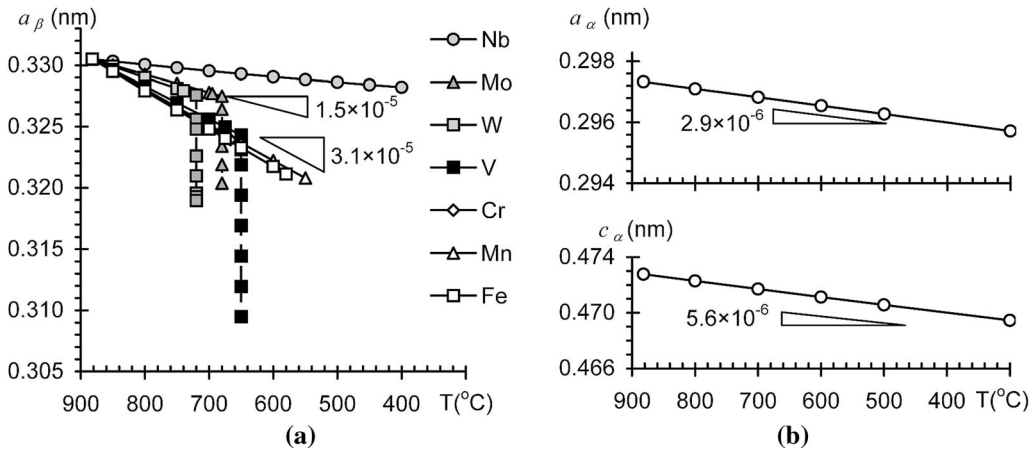

Fig. 4—Equilibrium lattice parameters for the (*a*) β or (*b*) α phase in binary titanium-β-stabilizer alloys in the (α + β) phase field.

the coefficient of thermal expansion of polycrystalline β titanium, and T is the temperature in °C. According to References 1, 32, 49, 50, the CTE is approximately independent of alloy content and varies with temperature as:

$$CTE \times 10^{6}[1/^{o}C] = 7.7 + 5.5 \times 10^{-3}(T - 20) \quad [2]$$

The temperature dependence of a_β for various binary titanium—β-stabilizer alloys is shown in Figure 4(a).

The α-phase lattice parameters $a_\alpha(T)$ and $c_\alpha(T)$ in titanium alloys at corresponding temperatures were determined using similar expressions,[1] *i.e.,*

$$a_\alpha(T) = a_\alpha^{RT}\left[1 + 9.928(T-25)10^{-6} - 0.626(T-25)^2 10^{-10}\right] \quad [3]$$

$$c_\alpha(T) = c_\alpha^{RT}\left[1 + 11.079(T-25)10^{-6} + 9.698(T-25)^2 10^{-10}\right], \quad [4]$$

in which a_α^{RT} and c_α^{RT} are the lattice parameters for HCP titanium at room temperature, and T is temperature in °C. The results of calculations using Equations (3) and (4) are shown in Figure 4(b). In model calculations, the effect of β stabilizers on the lattice parameters of the α phase was neglected due to their low solubility (Table II) and thus likely limited influence. Indeed, a solid solution of 3 at. pct V in the HCP titanium lattice leads to a decrease in both the a_α and c_α parameters (at room temperature) of less than 0.04 pct, while a solid solution of the same amount of V in the BCC lattice decreases a_β by more than 0.2 pct.[51,52]

A comparison of Figures 4(a) and (b) suggests a much faster decrease in the lattice parameter of the β phase in contrast to those of the α phase upon a decrease in temperature in binary titanium alloys. The largest changes in a_β are observed for alloys in the Ti-V system at a temperature ~ 20 °C below the monotectoid reaction during an "infinitely-long" annealing time (Figure 4(a)). Thus, it might be expected that Ti-V alloys would tend to exhibit atomic-spacing mismatch, α/β interface defect densities, and interface energies which vary over the widest range. Therefore, model calculations in the present work were focused on the Ti-V system at temperatures in the two-phase field down to 650 °C. In addition, a nominally-equilibrium condition was assumed in which the α phase did not contain β-stabilizing elements, and the vanadium concentration in the adjacent β phase $C(V)_\beta$ increased linearly from 1 at. pct at 870 °C to 20 at. pct at 650 °C. A further increase in $C(V)_\beta$ from 20 to 80 at. pct occurs during an "infinitely-long" soak of Ti-V alloys at a constant temperature of 650 °C.

B. *Effect of Vanadium Concentration in the β Phase on the Interface Structure*

As discussed in Section II, α/β interfaces in titanium alloys contain structural ledges and/or arrays of MDs of various types. These defects accommodate both misfit in interatomic (interplanar) spacing $f_{\mathbf{bi}}$ along the Burgers vectors $\mathbf{b_i}$ of the MDs and small angles between the mating planes and directions (Table I). In the first case, the value of misfit can be determined as $f_{\mathbf{bi}} = 2|a_i - b_i|/(a_i + b_i)$, where a_i and b_i are the interatomic distances in the α and β phases, respectively, along the i direction. In the second case, $f \approx \theta$. The periodicity p of MDs in each array is inversely proportional to the value of f.[13,28–31] Algorithms for evaluating the misfit (f), the spacing (p) between MDs of various types, and the periodicity of structural ledges (l) are described in general in References 13, 28, 29 and in particular for titanium alloys in Reference 31. The corresponding results for $f_{\mathbf{bi}}$, $p_{\mathbf{bi}}$, and l are shown in Figure 5.

Figure 5(a) shows that the misfit $f_{\mathbf{bi}}$ can either increase or decrease with increasing $C(V)_\beta$ depending on the crystallographic direction. Nevertheless, for any value of $C(V)_\beta$ (and at all temperatures of the $\beta \rightarrow \alpha$ diffusional transformation), $f_{\mathbf{bi}}$ does not exceed ~ 0.1 (10 pct) for any direction (Figure 2, Table I). According to References 6–8, the dislocation cores in any given array are not close to each other in such cases, and thus the dislocation lines can be distinguished on each face of the α/β interface.[17–27]

The spacing $p_{\mathbf{bi}}$ between misfit dislocations with the Burgers vector $\mathbf{b_i}$ (denoted as $\mathbf{b_i}$-MD) are shown in Figure 5(b). It should also be noted that the inter-dislocation spacing can vary by an order of magnitude in different arrays, *i.e.,* from several nanometers ($\mathbf{b_1}$-MDs, $\mathbf{b_4}$-MDs) to tens of nanometers ($\mathbf{b_2}$-MDs, $\mathbf{b_3}$-MDs, $\mathbf{b_z}$-TMDs). Depending on the temperature at which the α lamellae form in the β matrix and, therefore, on the vanadium concentration in the equilibrium β phase ($C(V)_\beta$), the average spacing between dislocations in each array can vary considerably (up to several times, Figure 5(b)). For example, the spacing between $\mathbf{b_2}$-MDs decreases by more than a factor of 6 while that between $\mathbf{b_4}$-MDs increases by 2.5 times. The spacing between dislocations, which accommodate the non-parallelism of the matching planes at the end face (Table I) is approximately 2.6 nm and changes very slightly with increasing $C(V)_\beta$ (not shown in Figure 5(b)), being mainly determined by the angle between the mating planes.[13]

With regard to the broad stepped boundary, the spacing between TMDs is inversely proportional to the misfit magnitude (*i.e.,* $f_{\mathbf{b1}}$ and $f_{\mathbf{bz}}$) in both the $\mathbf{b_1}$ and $\mathbf{b_z}$ directions, while the width of the structural ledges l on terraces is inversely proportional to the $f_{\mathbf{b1}}$ mismatch only.[28–31] The $f_{\mathbf{b1}}$ value gradually increases with increasing $C(V)_\beta$ over the entire range of concentrations considered, while $f_{\mathbf{bz}}$ first decreases to zero with increasing $C(V)_\beta$ to ~ 58 at. pct, and then increases again (Figure 5(a)). Calculations show (Figure 5(b)) that an increase in $C(V)_\beta$ from 1 to 25–30 at. pct does not change the spacing between TMDs considerably (p_{TMD} is about 30 nm), while the width of the terraces l decreases from ~ 1.3 to ~ 0.9 nm (and becomes 3 to 4.5 times the interatomic spacing), which is consistent with experimental results.[19,20] An increase in $C(V)_\beta$ from 30 to ~ 58 at. pct results in a rapid increase in the spacing of TMD to infinity, because the interplanar spacing along $[0\,\bar{1}\,1\,0]_\alpha || [1\,\bar{1}\,2]_\beta$ becomes similar. It worth noting that for the same value of $C(V)_\beta$, the terrace width of the structural ledges becomes close to the interatomic spacing in the $\mathbf{b_1} = 1/3[\bar{2}110]_\alpha || 1/2[\bar{1}11]_\beta$ direction, and the concept of a boundary with structural ledges loses physical meaning.[28,29] It can be readily shown that the width of terrace ledges exceeds two average-interatomic distances (which means that boundaries with structural ledges can exist) only if $f_{\mathbf{b1}} < 1/12 \approx 0.083$ or $a_\beta/a_\alpha > 1.062$, for which the value of the a_β/a_α ratio is given by the corresponding value of $C(V)_\beta$ in Figure 6.

The present data on the nature of structural defects at α/β interfaces in titanium alloys are in satisfactory agreement with experimental results[17–27] and therefore can be used with confidence to estimate interface energies. Moreover, the results can explain the reason for large scatter in experimentally-measured inter-dislocation distances along α/β interfaces which have been reported in different studies.

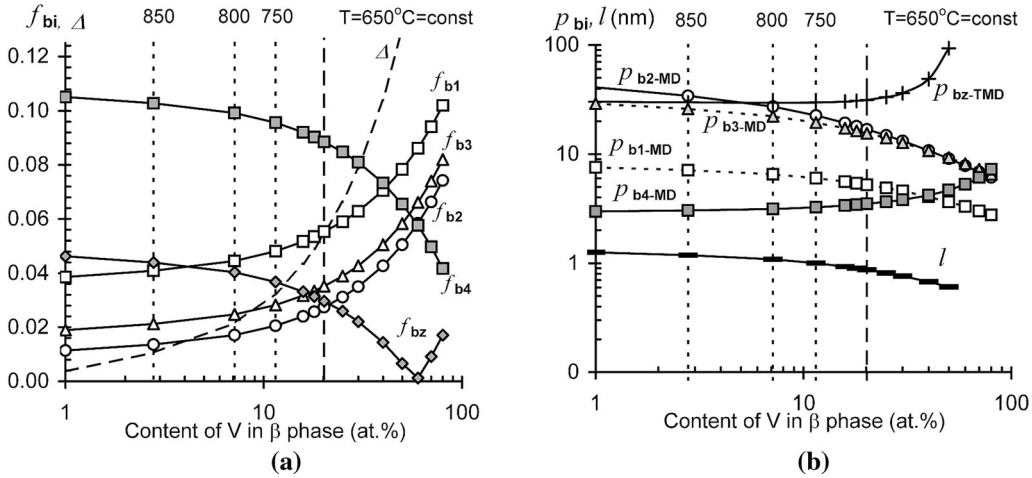

Fig. 5—Effect of V concentration in the β phase of titanium alloys on (*a*) interatomic misfit (f_{bi}) and volume difference (Δ) resulting from the $\beta \rightarrow \alpha$ transformation and (*b*) periodicity of interfacial misfit dislocations (p_{bi}) and structural ledges (l) at α/β interfaces.

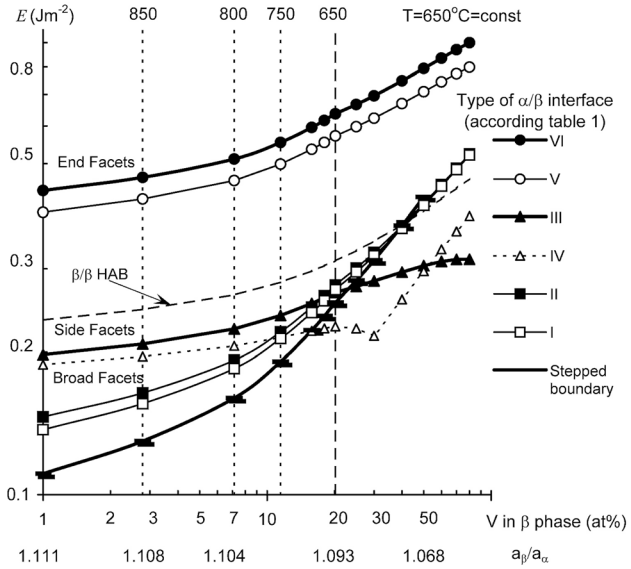

Fig. 6—Energy of α/β interfaces in Ti-V alloys as a function of the vanadium concentration.

C. *Effect of Temperature and Composition on Elastic Properties of the α and β Phases*

To calculate the interface energy in Ti-V alloys, the effect of temperature and $C(V)_\beta$ on elastic properties of both the β and α phases must be known. Because the vanadium content in the α phase is negligible (Section III–A), the shear modulus (μ_α) and the Poisson's ratio (ν_α) of the α phase depend only on temperature. The temperature dependence of μ_α and ν_α have been reported in References 53 through 55 and is summarized in Table III. In contrast, the elastic constants for the β phase (μ_β and ν_β) have been found to be weakly dependent on temperature.[54,55] However, they are sensitive to alloying-element content.[2,3,5] Table III shows the values of μ_β, μ_α, ν_β, and ν_α (at various values of $C(V)_\beta$ and corresponding $\beta \rightarrow \alpha$ transformation temperatures) calculated per the Voigt–Reuss–Hill method[56] using experimental data for solution-treated-and-quenched Ti alloys with different vanadium concentrations.[2]

IV. EFFECT OF THE VANADIUM CONTENT IN THE β PHASE (OR β → α TRANSFORMATION TEMPERATURE) ON THE α/β INTERFACE ENERGY

The energy of the β/α interfaces formed by different pairs of matching planes (Table I, Figure 2) was calculated using the relations described in detail in References 13, 15, 28–31. The results of the calculations (Figure 6) were also compared to the energy of a β/β grain boundary with a misorientation angle of 15 deg (denoted as β/β HAB). This β/β HAB energy was determined per the Reed–Shockley equation with $A_0 = 0$ (in which A_0 depends on the total core energy of the dislocation per unit area of the boundary)[57] and the μ_β and ν_β values given in Table III. Here, α/β interfaces whose energy is close to that of high-angle grain boundaries are assumed to be incoherent and, therefore, exhibit properties similar to those of an average high-angle grain boundary.[6–8] In other words, a similarity of the energies of high-angle grain boundaries and α/β interfaces is taken to be the criterion for a loss of interface coherency.

Per this criterion, the end faces of the α plates (type V, IV) (with three arrays of MDs of different types) are incoherent for any value of $C(V)_\beta$. That is to say, the energy of the end faces was calculated to be 0.4 to 0.9 J/m^2 which is typical of incoherent boundaries.[6–8,10,11,58]

The side faces (type III) form partly-coherent boundaries with an energy increasing from 0.2 to 0.3 J/m^2 for the range of $C(V)_\beta$ considered here. In this case, the energy of a high-angle grain boundary is 1.2 to 1.5 times that of the side faces. Broad faces with structural ledges have the lowest energy at relatively low values of $C(V)_\beta$ only; *i.e.*, at high transformation temperatures for which $a_\beta/a_\alpha > 1.097$. With an increase in $C(V)_\beta$, the broad-face

Table III. Elastic Moduli of the α and β Phases of Ti-V Alloys at Various $\beta \rightarrow \alpha$ Transformation Temperatures

T (°C)	870	850	800	750	700	675	650	650	650	650
$C(V)_\beta$ (At. Pct)	1	2.8	7.1	11.5	15.8	18.0	20.2	30	50	80
μ_β (GPa)	17.63	18.74	20.39	21.96	23.44	24.16	24.87	27.86	33.24	40.10
ν_β	0.397	0.393	0.387	0.382	0.378	0.376	0.374	0.368	0.359	0.353
μ_α (GPa)	19.83	20.60	21.80	23.00	24.20	24.80	25.40	25.40	25.40	25.40
ν_α	0.409	0.407	0.403	0.399	0.395	0.393	0.391	0.391	0.391	0.391

energy increases rapidly, and, for $C(V)_\beta \approx 18$ at. pct, it becomes close to the energy of either the broad face with a network of MDs (types I and II) or the energy of the side face (Figure 6). For $C(V)_\beta$ in the range of ~ 18 to ~ 30 at. pct (a_β/a_α decreasing from ~ 1.095 to ~ 1.085), the energy of the broad and side faces is ~ 0.26 J/m^2; *i.e.,* they differ from each other by only ~ 10 pct which is ~ 2.5 times less than the end-face energy. In this case, the formation of α phase which is acicular, as opposed to lamellar, can be expected, as has been observed for Ti-Fe system alloys annealed at 695 °C for 1032 hours ($a_\beta/a_\alpha \approx 1.0937$)[59] as well as some other titanium alloys with high β-stabilizer contents.[1–5] If $C(V)_\beta$ lies in the range between 20 and 40 at. pct, the boundary formed by $(0\bar{1}11)_\alpha$ and $(101)_\beta$ planes (type IV in Table I) has the lowest energy. In Figure 6, the dashed line for the energy of this matching facet is approximate because the predicted values have a significant error associated with the presence of partial dislocations at the boundary. In this regard, previous works[16,23] have shown very good matching between pairs of planes such as $(1\bar{1}01)_\alpha \| (1\bar{1}0)_\beta$ if the Pitsch–Schrader or the Potter OR is assumed.

For $C(V)_\beta \approx 40$ at. pct ($a_\beta/a_\alpha \approx 1.076$, $c_\alpha/a_\alpha \approx 1.588$), the energy of the broad face becomes equal to that of a high-angle grain boundary (~ 0.37 J/m^2), and, in accordance with the above criterion, the broad face formed by the $(0\ \bar{1}\ 10)_\alpha \| (1\ \bar{1}\ 2)_\beta$ planes is incoherent.

An increase in the vanadium concentration in the β phase with a decrease in the $\beta \rightarrow \alpha$ transformation temperature leads to not only an increase in the energy of the α/β interfaces, but also an increase in the transformation-volume parameter $\Delta = |V_\beta - V_\alpha|/V_\beta$ (Figure 5(a)). The value of Δ is ~ 0.5, ~ 5, or ~ 10 pct for $C(V)_\beta$ equal to 1, 18, and 40 at. pct, respectively. A significant volume effect impedes the phase transformation and results in the development of strain in the matrix.[6–8] In titanium alloys with a high β-stabilizer content, it is known[1,3–5] that α-phase precipitates form in β-solute-depleted areas developed by an initial solute-partitioning process.

The above reasoning for the structure and energy of α/β interfaces (Figures 5, 6) is valid not only for alloys of the Ti-V system, but also for any titanium alloy with β-stabilizers which reduce the lattice parameter of the β phase. In other alloys, the concentration of the alloying elements in the adjacent phases at each $\beta \rightarrow \alpha$ transformation temperature differs from the equilibrium value $C(V)_\beta$ shown in Figures 5 and 6. However, the misfit magnitude, the periodicity of defects along the matching facets, and the corresponding difference in energy is likely similar to the results in Figures 5 and 6 if the lattice-parameter ratio a_β/a_α ($c_\alpha/a_\alpha \approx 1.59$) is close to that for Ti-V alloys.

The effect of α-stabilizing and neutral elements on the α/β interface energy depends on the solubility of these elements in the phases and on the lattice parameters of the α and β phases. The addition of Al or Ga, both of which decrease the lattice parameter of the α phase,[1,52] leads to improved matching along the broad face and thus an energy reduction. By contrast, additions of Sn or Ag (each of which increases a_α and c_α) should have the opposite effect.

The present results suggest that the lamellar/acicular morphology of the α phase particles in the β matrix of titanium alloys is quite stable and globularization of the α phase is unlikely without deformation. Some modification in the compositions of the matrix phase caused either by alloying and/or temperature changes can influence the energy of α/β interfaces and therefore the kinetics of α-phase precipitation during heat treatment and its globularization during hot/warm deformation. Therefore the present data on the energy of interfaces is very useful for understanding the kinetics of structure evolution in two phase titanium alloys.

The present approach to calculate the α/β interface energy has some limitations, however. In particular, all of the calculated energy values contain a systematic error associated with the neglect of the energy associated with distortion of the second (and subsequent) layers of atoms. In addition, the energy values for the end face (type V, VI in Table I) are *overestimated*; this energy was obtained as a result of the algebraic summation of energies associated with three arrays of dislocations whose Burgers vectors are not perpendicular. In this case, the Burgers vectors have mutual parallel components, and the interaction energy is thus non-negligible.[15] The side face energy (type III), on the contrary, is somewhat *underestimated* because it does not consider the energy penalty due to the accommodation of the non-parallel $1/3[\bar{1}\bar{1}20]_\alpha$ and $[001]_\beta$ directions (*i.e.,* the screw component of the MDs). Last, the energy of a high-angle grain boundary may differ from that shown in Figure 6 if $A_0 \neq 0$ in the Reed–Shockley equation.[57] In spite of such possible shortcomings, the present dependences are

believed to provide semi-quantitative insight into the structural component of the energy of different faces between the α plates and β matrix due to the chemical composition of the phases and their corresponding lattice parameters.

V. CONCLUSIONS

An analysis of experimental data and simulations for the structure of interfaces between the α phase (HCP lattice) and β matrix (BCC lattice) in titanium alloys was performed. Pairs of crystallographic planes which can form different matching faces and retain the Burgers OR between the BCC and HCP lattices were selected.

For the broad or side faces consisting of $\left(0\ \bar{1}\ 10\right)_\alpha||\left(1\ \bar{1}\ 2\right)_\beta$ or $(0001)_\alpha||(110)_\beta$ planes, respectively, as well as for some facets of the end faces comprising non-parallel $\left(1\bar{1}00\right)_\alpha$ and $\left(1\bar{1}0\right)_\beta$ or $\left(1\bar{1}0\bar{1}\right)_\alpha$ and $\left(\bar{1}30\right)_\beta$ planes, the structural-ledge periodicity, misfit-dislocation periodicity, and the corresponding values of the α/β interface energy were determined. Enrichment of the β phase with substitutional β-stabilizing elements results in both a decrease in the a_β/a_α ratio and an increase in the energy of each of the faces.

For $a_\beta/a_\alpha > 1.10$ (pertaining to alloys with a small amount of β-stabilizing elements and temperatures high in the α/β phase field), a broad face with structural ledges has the lowest energy (0.1 to 0.2 J/m^2), while the anisotropy of the interface energy is greatest (*i.e.,* $E_{\text{End}}/E_{\text{Broad}} \approx 3$ to 4). This suggests that the lamellar shape of the α phase is stable during prolonged heating.

For $a_\beta/a_\alpha \approx 1.090 \pm 0.005$ (typical for near-β and β Ti alloys), the energies of the broad and side faces are similar to each other ($\sim 0.26 \pm 0.02$ J/m^2), and the $E_{\text{End}}/E_{\text{Broad}}$ anisotropy is lowest ($\approx$2.5). In these instances, the formation of α phase which is acicular is likely.

The boundaries formed by pairs of the planes $\left(0\bar{1}11\right)_\alpha||(101)_\beta$ have low energy (~ 0.3 J/m^2) and a partly coherent structure for $a_\beta/a_\alpha < 1.08$. This can result in a change in the orientation relationship between the α and β phases but does not lead to the formation of equiaxed-α, even if the broad face ($\left(0\ \bar{1}\ 10\right)_\alpha||\left(1\bar{1}\ 2\right)_\beta$) becomes incoherent ($a_\beta/a_\alpha \approx 1.076$, $E \approx 0.37$ J/m^2).

The main practical result of this theoretical analysis comprises the inability to bring about the precipitation of equiaxed α particles in the β phase irrespective of both the type/fraction of β stabilizers and heat treatment parameters.

ACKNOWLEDGMENTS

The present work was accomplished according to the state assignment of IMSP RAS. S.Z. and D.K gratefully acknowledge the financial support of the Russian Foundation for Basic Research under Grant No. 18-48-310023\18.

REFERENCES

1. U. Zwicker: *Titan und titanlegierungen*, Springer, Berlin, 1974, pp. 248–337.
2. E.W. Collings: *The Physical Metallurgy of Titanium Alloys*, ASM, Metals Park, OH, 1984.
3. G. Lütjering and J.C. Williams: *Titanium*, 2nd ed., Springer, Berlin, 2007, pp. 203–336.
4. S.L. Semiatin and D.U. Furrer: in *ASM Handbook, vol. 22, Fundamentals of Modeling for Metals Processing*, S.L. Semiatin and D.U. Furrer, eds., ASM International, Materials Park, OH, 2009, vol. 22, pp. 536–52.
5. D. Banerjee and J.C. Williams: *Acta Mater.*, 2013, vol. 61, pp. 844–79.
6. A. Kelly, G.W. Groves, and P. Kidd: *Crystallography and Crystal Defects*, Longman, London, 1970, pp. 365–406.
7. *Physical Metallurgy*, 22th ed., R.W. Cahn, and P. Haasen, eds., *Physical Metallurgy* , 4th ed., V.2. Elsevier Science BV, North-Holland, Amsterdam, 1996, pp. 1363–1496.
8. *Physical Metallurgy*, 4th ed., D.E. Laughlin, and K. Hono, eds., *Physical Metallurgy*, 5th ed., Newnes, Oxford, 2014, pp. 1317–1445.
9. M.I. Mazurski and G.A. Salishchev: *Phys. Status Solidi B*, 1995, vol. 187, pp. 501–09.
10. R. Shi, N. Ma, and Y. Wang: *Acta Mater.*, 2012, vol. 60, pp. 4172–84.
11. J.C. Da Teixeira, B. Appolaire, E. Aeby-Gautier, S. Denis, and F. Bruneseaux: *Acta Mater.*, 2006, vol. 54, pp. 4261–71.
12. N. Ma, F. Yang, C. Shen, G. Wang, G.B. Viswanathan, P.C. Collins, D. Xu, R. Yang, H.L. Fraser, and Y. Wang: in *Ti-2007 Science and Technology*, M. Ninomi, S. Akiyama, M. Ikeda, M. Hagiwara, and K. Maruyama, eds., The Japan Institute of Metals, Kyoto, 2007, pp. 287–90.
13. J.H. van der Merwe: *Proc. Phys. Soc. A*, 1950, vol. 63, pp. 616–37.
14. J.P. Hirth, G. Spanos, M.G. Hall, and H.I. Aaronson: *Acta Mater.*, 1998, vol. 46, pp. 857–68.
15. G.J. Shiflet: *Mater. Sci. Eng.*, 1986, vol. 81, pp. 61–100.
16. T. Furuhara and H.I. Aaronson: *Acta Metall. Mater.*, 1991, vol. 39, pp. 2857–72.
17. E.S.K. Menon and H.I. Aaronson: *Acta Metall.*, 1986, vol. 34, pp. 1975–81.
18. T. Furuhara, H.J. Lee, E.S.K. Menon, and H.I. Aaronson: *Metall. Trans.*, 1990, vol. 21A, pp. 1627–43.
19. T. Furuhara, J.M. Howe, and H.I. Aaronson: *Acta Metall. Mater.*, 1991, vol. 39, pp. 2873–86.
20. T. Furuhara, T. Ogawa, and T. Maki: *Phil. Mag. Lett.*, 1995, vol. 72 (3), pp. 175–83.
21. M.J. Mills, D.H. Hou, S. Suri, and G.B. Viswanathan: in *Boundaries and Interfaces in Materials: The David A. Smith Symposium*, R.C. Pond, W.A.T. Clark, A.H. King, and D.B. Williams, eds., TMS, Warrendale, PA, 1998, pp. 295–301.
22. S. Suri, G.B. Viswanathan, T. Neeraj, D.-H. Hou, and M.J. Mills: *Acta Mater.*, 1999, vol. 47, pp. 1019–34.
23. N. Miyano, K. Ameyama, and G.C. Weatherly: *Mater. Trans.*, 2002, vol. 43 (7), pp. 1547–51.
24. R.C. Pond, S. Celotto, and J.P. Hirth: *Acta Mater.*, 2003, vol. 51, pp. 5385–98.
25. F. Ye, W.-Z. Zhang, and D. Qiu: *Acta Mater.*, 2004, vol. 52, pp. 2449–60.
26. F. Ye and W.-Z. Zhang: *Acta Mater.*, 2006, vol. 54, pp. 871–79.
27. S. Nag, R. Banerjee, R. Srinivasan, J.Y. Hwang, M. Harper, and H.L. Fraser: *Acta Mater.*, 2009, vol. 57, pp. 2136–47.
28. J.H. van der Merwe, G.J. Shiflet, and P.M. Stoop: *Metall. Trans. A*, 1991, vol. 22A, pp. 1165–75.
29. J.H. van der Merwe and G.J. Shiflet: *Acta Metall. Mater.*, 1994, vol. 42, pp. 1173–87.
30. S. Zherebtsov, G. Salishchev, and S.L. Semiatin: *Philos. Mag. Lett.*, 2010, vol. 90, pp. 903–14.
31. M.A. Murzinova, S.V. Zherebtsov, and G.A. Salishchev: *J. Exp. Theor. Phys.*, 2016, vol. 122 (4), pp. 705–15.
32. J.W. Elmer, T.A. Palmer, S.S. Babu, and E.D. Specht: *Mater. Sci. Eng. A*, 2005, vol. 391, pp. 104–13.
33. S. Malinov, W. Sha, Z. Guo, C.C. Tang, and A.E. Long: *Mater. Charact.*, 2002, vol. 48, pp. 279–95.
34. A.A. Il'in, V.M. Maistrov, and V.V. Zasypkin: *Metallofizika*, 1986, vol. 8, No. 6, pp. 112–13 [in Russian].

35. A.A. Il'in, M.Yu. Kollerov, V.V. Zasypkin, V.M. Maistrov: *Metalloved. Termich. Obrab. Met*. 1986, No. 1, pp. 52–56 [in Russian].
36. P. Barriobero-Vila, G. Requena, T. Buslaps, M. Alfeld, and U. Boesenberg: *J. Alloys Compd*., 2015, vol. 626, pp. 330–39.
37. A.K. Swarnakar, O. Van der Biest, and B. Baufeld: *J. Alloys Compd*., 2011, vol. 509, pp. 2723–28.
38. J.L. Murray: Chromium – Titanium (1987), in: H. Baker, H. Okamoto eds., *ASM Handbook Vol. 3*: *Alloy Phase Diagrams*, ASM International, Materials Park, OH, 1998, pp. 709–10.
39. J.L. Murray: Iron—Titanium (1992), in: H. Baker, H. Okamoto eds., *ASM Handbook Vol. 3: Alloy Phase Diagrams*, ASM International, Materials Park, OH, 1998, pp. 869–70.
40. J.L. Murray: Manganese—Titanium (1987), in: H. Baker, H. Okamoto eds., *ASM Handbook Vol. 3: Alloy Phase Diagrams*, ASM International, Materials Park, OH, 1998, pp. 1133–34.
41. J.L. Murray: Molybdenum—Titanium (1987), in: H. Baker, H. Okamoto eds., *ASM Handbook Vol. 3: Alloy Phase Diagrams*, ASM International, Materials Park, OH, 1998, pp. 1156–57.
42. J.L. Murray: Niobium—Titanium (1987), in: H. Baker, H. Okamoto eds., *ASM Handbook Vol. 3: Alloy Phase Diagrams,* ASM International, Materials Park, OH, 1998, pp. 1193–94.
43. J.L. Murray, Titanium—Vanadium (1989), in: H. Baker, H. Okamoto eds., ASM Handbook Vol. 3: *Alloy Phase Diagrams*, ASM International, Materials Park, OH, 1998, pp. 1469–70.
44. J.L. Murray: Titanium—Tungsten (1987), in: H. Baker, H. Okamoto eds., *ASM Handbook Vol. 3: Alloy Phase Diagrams*, ASM International, Materials Park, OH, 1998, pp. 1470–71.
45. N.P. Lyakishev ed.: *Equilibrium Diagrams of Binary Metal Systems*. Reference Book, 3-Volume Set, Moscow, Engineering, 1996 [in Russian].
46. O. Nakano, H. Sasano, T. Suzuki, H. Kimura: *J. Jpn. Inst. Met*., 1981, vol. 45, No. 7, pp. 653–60.
47. R. Baloyi: M.S. Thesis, University of the Witwatersrand. Johannesburg, 2010. http://hdl.handle.net/10539/10621.
48. L.-C. Ming, M.H. Manghnani, and K.W. Katahara: *Acta Metall*., 1981, vol. 29, pp. 479–85.
49. O.N. Senkov, B.C. Chakoumakos, J.J. Jonas, and F.H. Froes: *Mater. Res. Bul*., 2001, vol. 36, pp. 1431–40.
50. V.E. Peletsky, V.Ya. Chekhovskoy, E.A. Belskaya: *Thermophysical properties of titanium and its alloys*, A.E. Sheindlin ed., Moscow, Metallurgy, 1985 [in Russian].
51. T.V. Pryadko: Metallofiz*Noveishie Tekhnol*., 2015, vol. 37 (2), pp. 243–55 [in Russian].
52. R.G. Innes: M.S. Thesis, US Air Force Institute of Technology (AFIT-SE), Wright-Patterson Air Force Base, Ohio, 1968. https://archive.org/details/DTIC_AD0835852/mode/2up.
53. E.S. Fisher and C.J. Renken: *Phys. Rev*., 1964, vol. 135 (2A), pp. A482–94.
54. H. Ogi, S. Kai, H. Ledbetter, R. Tarumi, M. Hirao, and K. Takashima: *Acta Mater*., 2004, vol. 52, pp. 2075–80.
55. O.N. Senkov, M. Dubois, and J.J. Jonas: *Metall. Mater. Trans. A*, 1996, vol. 27A, pp. 3963–70.
56. T.D. Shermergor: *Theory of Elasticity for Micro-nonhomogeneous Media*, Nauka, Moscow, 1977 [in Russian].
57. W.T. Read and W. Shockley: *Phys. Rev*., 1950, vol. 78 (3), pp. 275–89.
58. A.S. Gornakova and S.I. Prokofjev: *J. Mater. Sci*., 2020, vol. 55, pp. 9225–36.
59. A.S. Gornakova, B.B. Straumal, A.N. Nekrasov, A. Kilmametov, and N.S. Afonikova: *J. Mater. Eng. Perform*., 2018, vol. 27 (10), pp. 4989–92.